doi:10.1093/brain/aww055 BRAIN 2016: 139; 1649–1656 | 1649

BRAIN
A JOURNAL OF NEUROLOGY

REPORT

De novo PMP2 mutations in families with type 1 Charcot–Marie–Tooth disease

William W. Motley,[1,2] Paulius Palaima,[3,4] Sabrina W. Yum,[5] Michael A. Gonzalez,[6] Feifei Tao,[6] Julia V. Wanschitz,[7] Alleene V. Strickland,[6] Wolfgang N. Löscher,[7] Els De Vriendt,[3,4] Stefan Koppi,[8] Livija Medne,[9] Andreas R. Janecke,[10,*] Albena Jordanova,[3,4,*] Stephan Zuchner[6,*] and Steven S. Scherer[1,*]

[*]These authors contributed equally to this work.

We performed whole exome sequencing on a patient with Charcot–Marie–Tooth disease type 1 and identified a *de novo* mutation in *PMP2*, the gene that encodes the myelin P2 protein. This mutation (p.Ile52Thr) was passed from the proband to his one affected son, and segregates with clinical and electrophysiological evidence of demyelinating neuropathy. We then screened a cohort of 136 European probands with uncharacterized genetic cause of Charcot–Marie–Tooth disease and identified another family with Charcot–Marie–Tooth disease type 1 that has a mutation affecting an adjacent amino acid (p.Thr51Pro), which segregates with disease. Our genetic and clinical findings in these kindred demonstrate that dominant *PMP2* mutations cause Charcot–Marie–Tooth disease type 1.

1 Department of Neurology, Perelman School of Medicine, University of Pennsylvania, Philadelphia, Pennsylvania 19104, USA
2 Department of Medicine, Pennsylvania Hospital, University of Pennsylvania, Philadelphia, Pennsylvania 19107, USA
3 Molecular Neurogenomics Group, VIB Department of Molecular Genetics, University of Antwerp, Universiteitsplein 1, 2650-Antwerpen, Belgium
4 Laboratory of Neurogenetics, Institute Born-Bunge, University of Antwerp, Universiteitsplein 1, 2650-Antwerpen, Belgium
5 Department of Pediatrics, Division of Neurology, The Children's Hospital of Philadelphia, Philadelphia, Pennsylvania 19104, USA
6 Department of Human Genetics and Hussman Institute for Human Genomics, University of Miami, Miami, Florida 33136, USA
7 Department of Neurology, Medical University of Innsbruck, Austria
8 Department of Neurology, State Hospital of Rankweil, Rankweil, Austria
9 Individualized Medical Genetics Center, The Children's Hospital of Philadelphia, Philadelphia, Pennsylvania 19104, USA
10 Division of Human Genetics, Department of Pediatrics, Medical University of Innsbruck, Innsbruck, Austria

Correspondence to: Steven S. Scherer,
The Perelman School of Medicine at the University of Pennsylvania,
3 W. Gates, 3400 Spruce St.,
Philadelphia, PA 19104,
USA
E-mail: sscherer@mail.med.upenn.edu

Keywords: peripheral neuropathy; Charcot-Marie-Tooth disease; CMT, myelin P2 protein; PMP2

Abbreviations: CMT = Charcot–Marie–Tooth disease; HMSN = hereditary motor and sensory neuropathy

Received November 13, 2015. Revised January 15, 2016. Accepted January 25, 2016. Advance Access publication March 23, 2016

Introduction

Charcot–Marie–Tooth disease (CMT; also known as hereditary motor and sensory neuropathy; HMSN) is the name for inherited peripheral neuropathies that are not part of more complex syndromes. With an estimated prevalence of 1 in 2500 persons, CMT/HMSN is one of the most common neurogenetic diseases, and is subdivided according to clinical, electrophysiological, histological, and genetic features (Saporta *et al.*, 2011). CMT1/HMSN-I is a dominantly inherited demyelinating neuropathy; it is more common than CMT2/HMSN-II, and is characterized by an earlier age of onset (first or second decade of life), nerve conduction velocities <38 m/s in upper limb nerves, and segmental demyelination and remyelination with onion bulb formations in nerve biopsies (Scherer and Wrabetz, 2008). CMT2/HMSN-II is also dominantly inherited, but nerve conduction velocities are >38 m/s, and biopsies mostly show a loss of myelinated axons. Dominantly inherited neuropathies with conduction velocities that fall in-between the two forms are called dominant intermediate CMT (CMTDI) (Nicholson and Myers, 2006).

Most CMT1 patients have a *PMP22* (MIM: 601097) duplication; most of the rest have a mutation in one of four different genes [*MPZ* (MIM: 159440), *LITAF* (MIM: 603795), *EGR2* (MIM:129010), or *NEFL* (MIM: 162280)] or missense *PMP22* mutations (Fridman *et al.*, 2015). With the exception of *NEFL* (which is primarily expressed in neurons), these genes are robustly expressed in Schwann cells, so that mutations in them are thought to cause demyelination through cell-autonomous effects (the mutations produce their deleterious effects in Schwann cells) (Scherer and Wrabetz, 2008). Dominant mutations in 17 different genes cause CMT2; with the exception of *MPZ*, these mutations are thought to produce an axonal neuropathy through their cell-autonomous effects in neurons. While CMT2 is genetically heterogeneous, with many unknown causes yet to be identified, only a few kindred with CMT1 remain unsolved (Fridman and Murphy, 2014). Here we present two novel *de novo* *PMP2* (MIM: 170715, GenBank: NM_002677) mutations that co-segregate with disease in two families with CMT1.

Materials and methods

Protocol approvals and patient consents

Institutional review board approval was obtained from the University of Pennsylvania, the Children's Hospital of Philadelphia, the University of Antwerp, and the University of Innsbruck for these studies. Written informed consent was obtained from each patient who participated.

Clinical data and sample collection

Each family member was seen by one of the authors (S.S.S., S.W.Y., J.V.W., W.N.L., S.K., or A.J.) in an outpatient clinic, where clinical neurophysiology was also performed with standard methods. A sural nerve biopsy was performed as part of the Family 1 proband's prior diagnostic workup, at another institution, at age 17. We obtained the epoxy blocks, recut them, and imaged thin sections with standard electron microscopy techniques.

Whole exome sequencing and analysis

Genomic DNA was isolated from peripheral blood from all participants. Exome DNA was captured using the SureSelect, Human All Exon 5 50 Mb kit (Agilent) and sequenced on a HiSeq 2000 (Illumina). Paired-end reads of 100-bp length were generated and alignment and variant calls were made using BWA (Li and Durbin, 2010) and GATK software packages (McKenna *et al.*, 2010). Data were then imported into GEM.app, a web-based collaborative genome analysis tool (Gonzalez *et al.*, 2013), where variants were filtered to identify non-synonymous or splice site variants with low frequency in public databases (not present in NHLBI Exome Variant Server), high conservation scores [GERP (Genomic Evolutionary Rate Profiling) >4, PhastCons Score >0.9, or phyloP Score >1.5] and damaging scores in at least one of the following *in silico* predictors of mutation consequence (SIFT, PolyPhen-2 HumDiv, MutationTaster, MutationAssessor, LRT, or FATHMM). The *PMP2* variant was confirmed by bidirectional Sanger sequencing using forward (TGCAATTGACTTGCCTGAAA) and reverse (AGGAGTGAAACATGGGAGGA) primers.

Cohort screening

A CMT cohort consisting of 136 probands was screened for variants in *PMP2* by Sanger sequencing. The four exons and their exon-intron boundaries were amplified using primers designed in Primer3 v4.0.0 (exon 1: forward 5′-agccttgcaaaactccc-cag–3′, reverse 5′-ttgcttagtcccgacactgc-′3; exon 2: forward 5′-tgtctcaggaggtacactcc-3′, reverse 5′-ccactgagcgtaggatgtgg-3′; exon 3: forward 5′-aaaatcttgggtcagtacttga-3′, reverse 5′-tggttcca-tactgaaagaactgc-3′; exon 4: forward 5′-ctcctctggcccctgtca-3′, reverse 5′-actggagactgacatactgat-3'). The PCR products were then purified using ExoSAP-IT® (USB) and bidirectionally sequenced using BigDye® Terminator v3.1 Cycle Sequencing kit (Applied Biosystems) on an ABI3730xl DNA Analyzer (Applied Biosystems). The acquired sequences were then aligned with SeqMan II (DNASTAR Inc.) to the *PMP2* reference sequence (GenBank accession number CH471068.1, NM_002677, NP_002668.1) obtained from UCSC Genome Browsers GRCh37 (hg19) human genome assembly (http://genome-euro.ucsc.edu/index.html).

Paternity testing and haplotype analysis

To confirm paternity in Family 1, segregation of five short tandem repeat polymorphic sites in the HLA locus (D6S265,

D6S1552, D6S1517, D6S1260, and MOG-CA) was checked by fragment length analysis using a multiplex fluorescent polymerase chain reaction (PCR) and capillary electrophoresis on an ABI3730 analyzer (Applied Biosystems) and analysed with GeneMapper 4.0 software (Applied Biosystems) (Fernández *et al.*, 2013). The same technique was used for haplotype analysis in Family 2, with five short tandem repeat polymorphic sites flanking the *PMP2* locus (D8S2321, D8S1738, D8S275, D8S525, D8S1697).

Control analysis

Samples from 188 anonymous blood donors from Western Austria were tested for the presence of the c.151A > C nucleotide (p.Thr51Pro) variant detected in Family 2 by PCR amplification of *PMP2* exon 2 using M13 sequence-tagged primers (PMP2_2fneu_M13f 5′-gtaaaacgacggccagtACCTGCCATCAACTCACCTG and PMP2_2r_M13r 5′-caggaaacagctatgacTAGATGTCTCAGGAGGTACACTCC) generating a 441-bp fragment using the following PCR cycling parameters: 1 × (95° 3 min) + 35 × (95° 20 s/58° 20 s/72° 20 s) + 1 × (72° 7 min) + 1 × (25° 1 min). The c.151A > C nucleotide variant abolishes a PstI restriction enzyme cutting site, and aliquots of PCR products were incubated with PstI restriction enzyme for 12 h at 37 °C in the appropriate buffer supplied by the manufacturer (New England Biolabs).

PCR products amplified from patient samples served as positive controls. Samples from controls were all completely cut into two fragments of 202-bp and 239-bp in size, whereas samples from positive controls were only partially cut, as resolved by agarose gel electrophoresis. The absence of the c.151A > C nucleotide variant among this cohort of controls further indicates that it is not a frequent polymorphism (Collins and Schwartz, 2002). Additionally, samples from 180 unaffected European individuals were screened by Sanger sequencing using the protocol described above.

Mutation mapping

Our description of the mutations follows HGVS nomenclature guidelines (http://www.hgvs.org/mutnomen) and is based on sequence from RefSeq Transcript NM_002677. The PMP2 protein sequences were aligned using the ClustalW2 sequence alignment tool (http://europepmc.org/abstract/MED/17846036). The PMP protein structure was downloaded from The Protein Data Bank (Berman *et al.*, 2000) (accession number 2WUT; Majava *et al.*, 2010) and viewed and annotated using the PyMol software (www.pymol.org).

Results

PMP2 mutations in two families with CMT1

We performed whole-exome sequencing (WES) as an unbiased approach to find the causal mutation in an unsolved family with CMT1 (Family 1). Prior to his arrival in our clinic, the proband had a commercial test (Athena Diagnostics) for all of the known causes of CMT1 [*PMP22*, *MPZ*, *GJB1* (MIM:304040), *EGR2*, *LITAF* and *NEFL*] as well as *MFN2* (MIM: 608507), *PRX* (MIM: 605725), *SH3TC2* (MIM: 608206), *GDAP1* (MIM: 606598), *GARS* (MIM: 600287), *HSPB1* (MIM: 602195), and *DNM2* (MIM: 602378). All of these were normal except for a synonymous c.234G > A variant in *LITAF*.

Exome sequencing identified 49 candidate variants in the proband that met the filtering criteria described above (Supplementary Table 1), one of which was a novel variant c.155T > C in *PMP2* (Fig. 1B). This variant was a strong candidate because *PMP2* encodes myelin protein P2, which is a constituent of compact myelin (Trapp *et al.*, 1984). The proband's parents and his living siblings do not have the disease, and bidirectional Sanger sequencing revealed that they do not carry the variant. Among the three sons of the proband, only the son with CMT1 was found to carry the *PMP2* variant (Fig. 1A and B). Paternity was confirmed for all living members of the second generation (Subjects II.2, II.3 and II.4). Segregation analysis combined with confirmation of paternity establishes that this mutation arose *de novo* in the proband and was transmitted as a dominant trait in his progeny.

To provide further genetic evidence for an association between *PMP2* variants and CMT1, we screened a cohort of 136 European probands from families with dominantly inherited CMT without a known genetic cause for mutations in *PMP2* with Sanger sequencing (104 with CMT1, 14 with CMTDI, two with hereditary neuropathy with liability to pressure palsies, three with hereditary motor neuropathy, and 13 with unspecified CMT). We identified a c.151A > C variant in *PMP2* in an Austrian family with CMT1. Bidirectional Sanger sequencing showed that the proband (Subject III.3), her two older affected sisters (Subjects III.1 and III.2), her affected mother (Subject II.3), her daughter (Subject IV.5), and her niece (Subject IV.1) carry the c.151A > C variant in *PMP2*. The proband's uncle (Subject II.2) and two aunts (Subjects II.1 and II.4) are unaffected and do not carry the mutation. The proband's maternal grandparents are deceased, but showed no signs of neuropathy. Haplotype analysis in all available family members in generation II and III of five short tandem repeat markers flanking the *PMP2* locus revealed that the c.151A > C variant arose *de novo* in Patient II.3 and was transmitted in a dominant fashion in her progeny (Supplementary Fig. 1).

The c.155T > C and c.151A > C variants are not present in the ~7000 exomes in the GEM.app database, renamed GENESIS, in the NHLBI Exome Variant Server, 1000 Genomes, the Genome Variant Database for Human Disease, nor ExAC. One hundred and eighty-eight healthy control subjects from Western Austria (ethnically matched to Family 2) were screened for the c.151A > C nucleotide variant detected in Family 2 using a restriction endonuclease site assay. The disease-associated variant eliminates a PstI restriction site. None of the PCR products amplified from genomic DNA of control samples had lost the PstI endonuclease site, indicating that none contained the

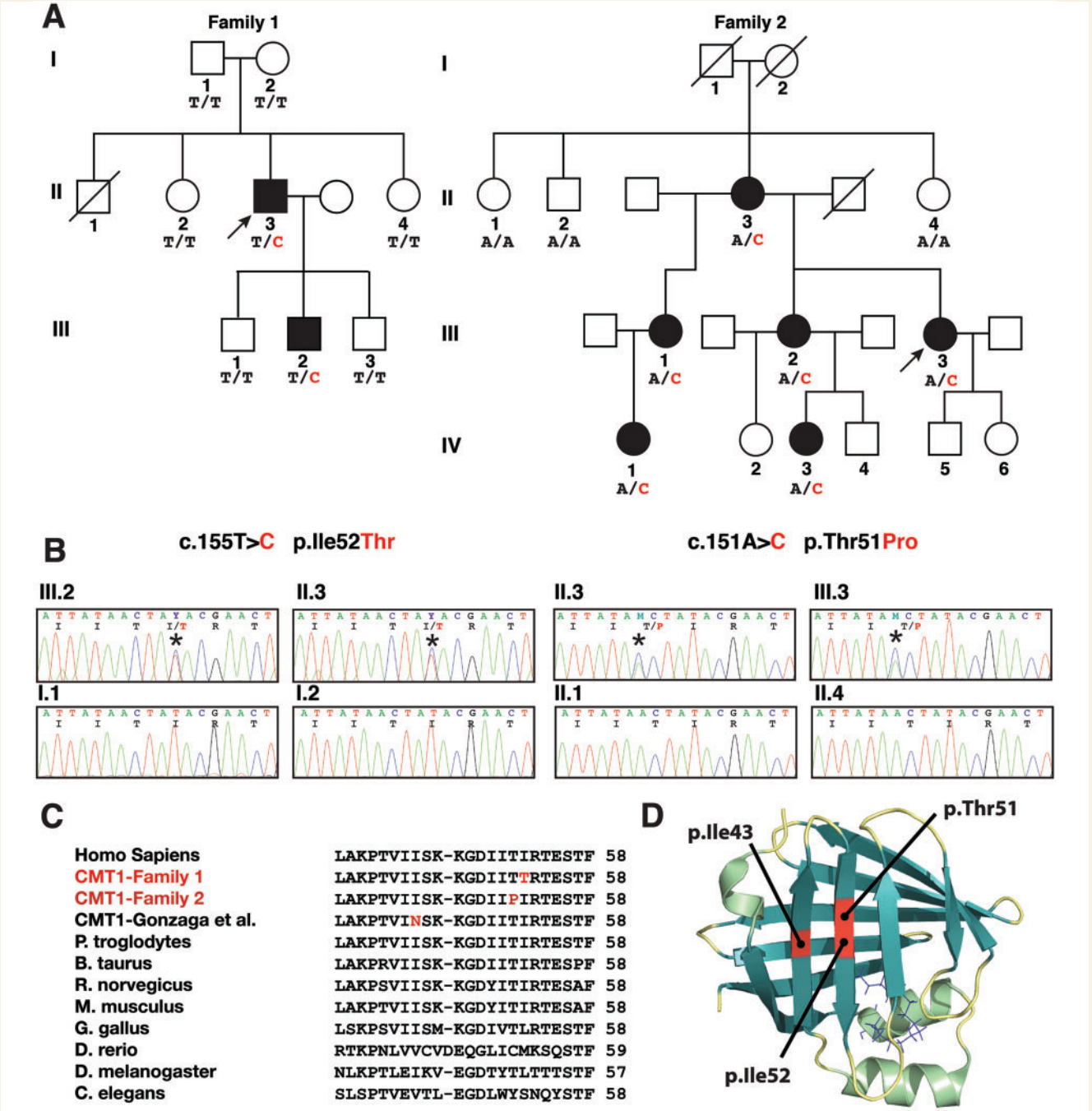

Figure 1 ***De novo PMP2*** **mutations segregate with disease in two families with CMT1.** In Family 1, a c.155T > C mutation segregates with CMT1 and affects a conserved amino acid in the beta barrel of P2. (**A**) Whole exome sequencing of our proband Subject II.3 identified a c.155T > C substitution. A candidate screen for mutations in families with CMT identified a c.151A > C mutation in Family 2. The genotypes of individuals whose DNA was collected and Sanger sequenced is shown below pedigree symbols. In Family 1, neither parent has any clinical evidence of neuropathy and neither harbours the mutation. One of the proband's sons is affected (Subject III.2) and harbours the mutation. In Family 2 the c.151A > C mutation segregates with CMT1 and affects a conserved amino acid adjacent to the mutation in Family 1. In Family 2, the proband (Subject III.3), her mother (Subject II.3), her two sisters (Subjects III.1 and III.2), and two nieces (Subjects IV.1 and IV.5), all show clinical features of neuropathy and carry the mutation, while the proband's two aunts and one uncle do not have neuropathy and do not carry the mutation. The proband's maternal grandparents are deceased, but did not show any signs of neuropathy. (**B**) Normal Sanger sequencing traces of the *PMP2* gene are shown from the Family 1 proband's parents, who are both unaffected, suggesting that the mutation arose *de novo* in our proband, and was passed onto his affected son. Sanger sequencing traces from the proband and her mother show the mutation in Family 2, while the proband's unaffected uncle and aunt do not have the mutation. (**C**) ClustalW2 alignments of the myelin P2 protein from divergent species. The p.Ile43Asn, p.Thr51Pro, and p.Ile52Thr CMT1-associated variants disrupt amino acid residues that are conserved in mammals, but are not present in teleosts or invertebrates. (**D**) The crystal structure of the P2 protein is shown modelled with a bound palmitate. Helical structures are shown in light green and beta strands are shown in teal. The three CMT1-associated variants are shown, and they cluster in adjacent positions of beta strand B (p.Ile43Asn) and beta strand C (p.Thr51Pro, and the p.Ile52Thr).

disease-associated variant. In addition, exon 2 of the *PMP2* gene was sequenced in 180 unaffected individuals of European descent; neither variant was identified in any of these control DNA samples. This provides further evidence that the variants identified in our families are not common polymorphisms (Collins and Schwartz, 2002).

The c.155T > C nucleotide variant is predicted to result in a missense substitution of the isoleucine residue at position 52 with a threonine (p.Ile52Thr or I52T), representing a change from a hydrophobic side chain to a polar side chain. The c.151A > C nucleotide variant is predicted to result in a missense threonine-to-proline substitution of the adjacent amino acid (p.Thr51Pro or T51P), representing a change from a polar uncharged side chain to a structurally rigid side chain. The PMP2 protein sequences from divergent species were aligned using the ClustalW2 sequence alignment tool (Larkin *et al.*, 2007). Both p.Ile52Thr and p.Thr51Pro lie in a domain of the protein that is well conserved in mammals (Fig. 1C), and they are close to the isoleucine residue at position 43 that has been recently proposed as a putative pathogenic mutation in another family with CMT1 (p.Ile43Asn or I43N) (Gonzaga-Jauregui *et al.*, 2015).

The PMP2 crystal structure consists of 10 anti-parallel beta strands, which compose two orthogonal beta pleated sheets that form a beta barrel. This beta barrel is the ligand-binding core surrounded by a hydrophilic surface (Ruskamo *et al.*, 2014). The isoleucine residues 43 and 52 occupy the same position on adjacent anti-parallel beta strands in the crystal structure (Fig. 1D).

Clinical features of PMP2-associated demyelinating neuropathy in two families

Family 1

The proband of Family 1 (Fig. 1) was diagnosed by an orthopaedic surgeon in his late teens after his feet were examined. At the time, he had a foot drop and reported increased falls. Nerve conduction studies at ages 17 and 32 showed slowed (~20 m/s) motor and sensory responses with reduced amplitudes. When first seen in our clinic at age 48, he was using moulded ankle foot orthoses. Strength, bulk, and tone were normal in the proximal muscles of his arms and legs. There was no movement of his extensor hallucis longus (0/5; MRC scale), severe weakness in ankle dorsiflexion (4−/5), and normal strength in ankle plantar flexion (5/5). Strength was normal in the finger extensors and the ulnar innervated intrinsic hand muscles, but there was marked weakness (4−/5) and atrophy in his bilateral abductor pollicis brevis (Supplementary Fig. 2). He was areflexic at the ankles, knees, and biceps. Vibratory sensation (scored using a Rydell-Seiffer tuning fork) was absent at the toes, 3 at the ankles, and 6 at the knees. Pinprick sensation was reduced to the calves, but present at the knees. Nerve conduction studies showed absent sensory responses, marked slowing and reduced amplitudes of motor responses (Table 1), and electromyography showed evidence of severe, chronic denervation in distal muscles. His CMT Neuropathy Score (version 2) (Murphy *et al.*, 2011) was 14. A sural nerve biopsy was performed as part of the proband's prior diagnostic workup at another institution at age 17 years. We obtained the epoxy blocks, recut them, and examined sections by light and electron microscopy. The density of myelinated axons was reduced; there were thinly myelinated (presumably remyelinated) axons, and some examples of onion bulbs (Fig. 2). A brain MRI without contrast at age 48 was normal and showed no intracranial white matter pathology (Supplementary Fig. 3).

Table 1 Nerve conduction studies of affected patients

	Family 1 Subject II.3 Age 46		Family 1 Subject III.2 Age 13		Family 2 Subject IV.1 Age 24		Normal values	
Sensory	**μV**	**m/s**	**μV**	**m/s**	**μV**	**m/s**	**μV**	**m/s**
Radial	NR	NR	NR	NR	NR	NR	⩾15	⩾50
Median[a]	NR	NR	NR	NR	NR	NR	⩾10	⩾50
Ulnar[a]	NR	NR	ND	ND	NR	NR	⩾7	⩾50
Motor[b]	**mV**	**m/s**	**mV**	**m/s**	**mV**	**m/s**	**mV**	**m/s**
Peroneal	ND	ND	NR	NR	ND	ND	⩾2.0	⩾41
Median	1.1	17	2.2	12.6	NR	NR	⩾4.0	⩾49
Ulnar	3.3	21	4.1	14.3	1.5	11.7	⩾6.0	⩾49

[a]Orthodromic;
[b]The amplitudes of the distal motor responses are shown.
NR = no response; ND = not done.

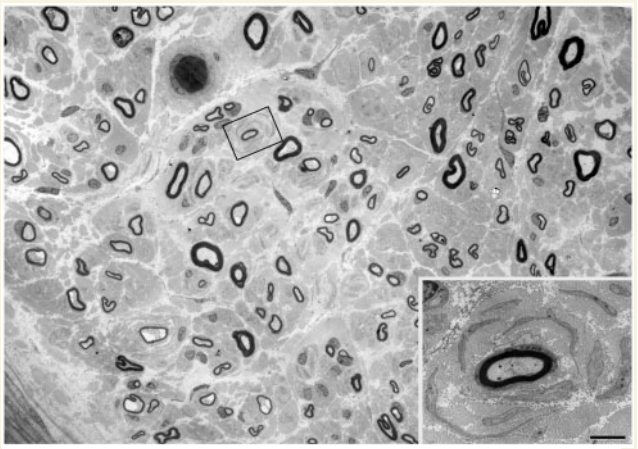

Figure 2 Sural nerve biopsy from the proband in Family 1. Digital electron micrograph from the sural nerve biopsy of the proband (Patient II.3) at age 17. The density of myelinated axons is reduced, but actively degenerating myelinated axons were not seen. Some of the myelinated axons had myelin sheaths that were inappropriately thin for the axon diameter, and some rudimentary onion bulbs were seen; one of which is indicated in the boxed region. There is increased endoneurial collagen. The inset is a higher magnification image of the boxed region, showing a thinly myelinated axon surrounded by Schwann cell processes. Scale bar = 1 μm.

The proband and his wife first noted that their second son was less nimble and coordinated than his peers at age 3, and subsequently developed difficulty going up stairs and getting up after falls. His exam at age 13 was notable for high arched feet and thin calves. He had decreased bulk in extensor digitorum brevis and intrinsic foot muscles, and reduced strength in extensor hallucis longus (3/5), ankle dorsiflexion (3/5), and ankle eversion (3/5); foot inversion and plantar flexion were normal (5/5). Strength in upper extremities, including in intrinsic hand muscles, was normal. Vibratory sensation was reduced at the toes, ankles, and knees; pinprick, and temperature sensation were decreased below the knees. Reflexes were absent at knees and ankles, and trace in the arms. Sensory responses were absent, and motor responses had mildly reduced amplitudes and marked slowing (Table 1); electromyography was not done. His CMT neuropathy score version 2, was 12. The other living members of the Family 1 were examined (by S.S.S. or S.W.Y.), and showed no evidence of neuropathy; Subject II.1, who was recently deceased, had no known manifestations of neuropathy.

Family 2

The proband in Family 2 (Fig. 1) was seen in clinic at age 20 for genetic counselling. At age 5, she was bothered by frequent tripping and distal lower extremity weakness. By age 11, she had developed high arched feet, thin calves, and hammertoes, and required an Achilles tendon lengthening surgery. At age 20, motor and sensory potentials were not detectable in her legs; electrophysiological studies 7 years prior had shown absent sensory responses and evidence of chronic denervation (large polyphasic motor units) in the tibialis anterior. The proband reported that her two older sisters (Subjects III.1 and III.2), mother (Subject II.3), and niece also had progressive weakness and were diagnosed with CMT. Her eldest sister (Subject III.1) and their mother (Subject II.3) were more mildly affected. The proband was seen again at age 37. She had worked as a truck driver but retired at 33 years of age. She has severe atrophy of calf, peroneal, and foot muscles, with severe weakness (0/5) in extensor halluces longus as well as foot inversion, dorsiflexion, and plantar flexion. There is also atrophy and weakness of intrinsic hand muscles, with the abductor pollicis brevis most affected. Deep tendon reflexes were absent in the lower extremities and trace in the upper extremities. There was evidence of mild sensory loss on clinical examination, without trophic disturbances. She walks with difficulty due to bilateral pes equinovarus. The proband has two daughters and one son. Her one affected daughter (Subject IV.5) was seen at age 13, with difficulty walking due to pes equinovarus as well as weakness and atrophy of calf, peroneal, and foot muscles. Strength was 4/5 or 5/5 in the intrinsic hand muscles. Reflexes were absent in the legs and normal in the arms. There was no sensory loss evident on clinical examination.

The proband's niece (Subject IV.1) was recently seen in clinic at age 24. Her walking was delayed (she started walking at 18 months) and subsequently she had difficulty walking due to pes equinovarus that was surgically corrected at age 8. Since then her motor deficits stabilized and she can walk unassisted for half an hour on flat terrain. She reported no impairment of her hand function. She reported mild numbness in her feet, without neuropathic pain. Her exam was notable for surgically corrected pes equinovarus without additional deformities in her hands or feet (Supplementary Fig. 2). She had severe atrophy of calf, peroneal, and foot muscles, with moderately high arches. Proximal leg muscles were strong, while there was reduced strength in foot inversion (0/5), extensor hallucis longus (0/5), foot dorsiflexion (1/5), and plantar flexion (4/5). Proximal arm muscles were strong, with mild atrophy and weakness (3–4/5) in her interosseous muscles and moderate atrophy and severe weakness (1/5) of abductor pollicis brevis. Vibratory and pin prick sensation were reduced in her arms and legs. Deep tendon reflexes were absent in the arms and legs and plantar reflexes were flexor. Nerve conduction studies showed absent sensory responses and absent median motor response; the ulnar motor response had a severely reduced amplitude and was severely slowed (Table 1). The proband's older (affected) sister (Subject III.2) had a brain MRI at age 37, which was normal (Supplementary Fig. 3).

Discussion

Our description of two *de novo* dominant disease-associated mutations in the *PMP2* gene confirm and extend the recent report of a candidate mutation in *PMP2* (p.Ile43Asn) as the cause of CMT1 (Gonzaga-Jauregui *et al.*, 2015). The p.Ile43Asn mutation segregated with the CMT phenotype in a family in four individuals. The proband's age of onset was 6 years, and his disease phenotype includes foot deformities, distal atrophy, sensory loss, and loss of deep tendon reflexes. His tibial motor response had reduced amplitude and was severely slowed (18 m/s), and a biopsy showed demyelinating neuropathy with onion bulb formation. Thus, all three reported *PMP2*-associated mutations share similar clinical and electrophysiological characteristics. Family 1 is part of a cohort of ~200 families with type 1 and type 2 CMT. Of those families, only the family presented in this work has a dominantly inherited CMT1 without a known genetic cause. Family 2 was identified in a screen of 136 European probands, of whom 104 have been diagnosed with CMT1 and do not have mutations in the most common CMT1 genes. Based on this, we believe that *PMP2* mutations are a rare cause of dominantly inherited CMT1 accounting for ~1% of CMT1 in cases where standard genetic testing has been negative, but further studies will be needed to confirm this preliminary observation. Our analysis shows that the three mutations affect amino acids that are predicted to be clustered near each other in the crystal structure of P2, but how they affect the function of the P2 protein is unknown.

Myelin protein zero (P0, or MPZ), myelin basic protein (P1, or MBP), and peripheral myelin protein 2 (P2, or PMP2) were originally described as the three major proteins in peripheral nervous system myelin (Greenfield *et al.*, 1973). Like other myelin-related genes, *Pmp2* mRNA expression is regulated by axon–Schwann cell interactions in rodents (Barrette *et al.*, 2010). P2 is a member of the fatty acid binding protein family and plays a role in intracellular trafficking of lipids: P2 binds fatty acids in the cytoplasm and transports them to vesicles and cell membranes, releasing them into the membrane when the protein becomes bound to it (Zenker *et al.*, 2014). Peripheral nervous system myelin contains much more P2 than does CNS myelin (DeArmond *et al.*, 1980; Kadlubowski *et al.*, 1984); this could account for the lack of clinical findings in our patients that would be typical of leukodystrophies (e.g. spasticity and optic atrophy).

Gonzaga-Jauregui *et al.* (2015) examined the effects of the p.Ile43Asn mutation in a zebrafish model by knocking down the expression of the endogenous *pmp2* mRNA (with a morpholino injection) and overexpressing either the wild-type or mutant human *PMP2*. Suppressing the endogenous P2 expression resulted in defective motor axon outgrowth that was rescued by wild-type but not the p.Ile43Asn P2 protein. This functional assay, however, is an experimental test of how gene deficiency affects motor neurons and their developing axons; its relevance as an *in vivo* model for the pathogenicity of the p.Ile43Asn variant in CMT1 is doubtful because (i) it does not mimic the dominant nature of *PMP2* mutation; and (ii) there is no evidence that axonal outgrowth is affected in human patients with any form of CMT1, including people with *PMP2* mutations.

It is much more plausible that the p.Ile43Asn, p.Thr51Pro, and p.Ile52Thr mutants result in a toxic gain of function in myelinating Schwann cells to cause demyelination. *Pmp2*-null mice have a mild phenotype (Zenker *et al.*, 2014), so a dominant-negative mechanism (Gonzaga-Jauregui *et al.*, 2015) may not be the relevant effect of the p.Ile43Asn, p.Thr51Pro, or p.Ile52Thr mutants. Dominant *SPTLC1* and *SPTLC2* mutations provide an illuminating example. Missense mutations in these genes, both membrane lipid binding proteins, cause a dominantly inherited neuropathy (hereditary sensory neuropathy 1A), likely by causing the misincorporation of glycine and alanine into sphingolipids that are toxic (Garofalo *et al.*, 2011; Scherer, 2011). While mutations in at least two domains in *SPTLC1* have been associated with HSAN1A, they cluster in subunits whose mutation allows incorporation of deoxysphingoid bases (Rotthier *et al.*, 2010). With just three candidate mutations identified, we have already observed tight structural clustering that suggests there may be a similar pathogenic mechanism; perhaps the p.Ile43Asn, p.Thr51Pro, and p.Ile52Thr PMP2 mutants alter the lipid binding pocket of P2 and result in aberrant transport of fatty acids and alteration in the lipid composition of compact myelin. This idea fits with prior data showing Schwann cells are very sensitive to perturbations in membrane lipid composition (Chrast *et al.*, 2011).

Acknowledgements

The authors would like to thank the families for their participation in this study. The authors would like to thank Jian Li for technical assistance with the electron microscopy. The authors would like to thank Steven Glynn for his help with PyMol renderings.

Funding

This work was supported by U54 NS065712 and the Judy Seltzer Levenson Memorial Fund for CMT Research. The authors would like to thank the families for their participation in this study. This study was funded in part by the University of Antwerp (TOP BOF 29069 to A.J.) and the Fund for Scientific Research-Flanders (FWO; to A.J.). P.P. is supported by a Ph.D. fellowships from the Research Fund of the University of Antwerp. The INC (U54NS065712) is a part of the NCATS Rare Diseases Clinical Research Network (RDCRN). RDCRN is an initiative of the Office of Rare Diseases Research (ORDR), NCATS, funded through a collaboration between NCATS and the NINDS.

Supplementary material

Supplementary material is available at *Brain* online.

Web resources

URLs for data presented herein are as follows:
GEM.app (renamed GENESIS): https://genomics.med.miami.edu/
1000 Genomes, http://www.1000genomes.org/
ExAC Browser, http://exac.broadinstitute.org
NHLBI Exome Sequencing Project Exome Variant Server, http://evs.gs.washington.edu/EVS/
OMIM, http://www.omim.org/
PyMol: (www.pymol.org)

Accession numbers

PMP2 (MIM: 170715, GenBank: NM_002677).

References

Barrette B, Calvo E, Vallières N, Lacroix S. Transcriptional profiling of the injured sciatic nerve of mice carrying the Wld(S) mutant gene: identification of genes involved in neuroprotection, neuroinflammation, and nerve regeneration. Brain Behav Immun 2010; 24: 1254–67.

Berman HM, Westbrook J, Feng Z, Gilliland G, Bhat TN, Weissig H, et al. The protein data bank. Nucleic Acids Res 2000; 28: 235–42.

Chrast R, Saher G, Nave K-A, Verheijen MHG. Lipid metabolism in myelinating glial cells: lessons from human inherited disorders and mouse models. J Lipid Res 2011; 52: 419–34.

Collins JS, Schwartz CE. Detecting polymorphisms and mutations in candidate genes. Am J Hum Genet 2002; 71: 1251–2.

DeArmond SJ, Deibler GE, Bacon M, Kies MW, Eng LF. A neurochemical and immunocytochemical study of P2 protein in human and bovine nervous systems. J Histochem Cytochem 1980; 28: 1275–85.

Fernández RM, Peciña A, Lozano-Arana MD, García-Lozano JC, Borrego S, Antiñolo G. Novel one-step multiplex PCR-based method for HLA typing and preimplantational genetic diagnosis of β-Thalassemia. Biomed Res Int 2013; 2013: 585106–9.

Fridman V, Bundy B, Reilly MM, Pareyson D, Bacon C, Burns J, et al. CMT subtypes and disease burden in patients enrolled in the Inherited Neuropathies Consortium natural history study: a cross-sectional analysis. J Neurol Neurosurg Psychiatr 2015; 86: 873–8.

Fridman V, Murphy SM. The spectrum of axonopathies: from CMT2 to HSP. Neurology 2014; 83: 580–1.

Garofalo K, Penno A, Schmidt BP, Lee H-J, Frosch MP, Eckardstein von A, et al. Oral l-serine supplementation reduces production of neurotoxic deoxysphingolipids in mice and humans with hereditary sensory autonomic neuropathy type 1. J Clin Invest 2011; 121: 4735–45.

Gonzaga-Jauregui C, Harel T, Gambin T, Kousi M, Griffin LB, Francescatto L, et al. Exome sequence analysis suggests that genetic burden contributes to phenotypic variability and complex neuropathy. Cell Rep 2015; 12: 1169–83.

Gonzalez MA, Lebrigio RFA, Van Booven D, Ulloa RH, Powell E, Speziani F, et al. GEnomes Management Application (GEM.app): a new software tool for large-scale collaborative genome analysis. Hum Mutat 2013; 34: 842–6.

Greenfield S, Brostoff S, Eylar EH, Morell P. Protein composition of myelin of the peripheral nervous system. J Neurochem 1973; 20: 1207–16.

Kadlubowski M, Hughes RA, Gregson NA. Spontaneous and experimental neuritis and the distribution of the myelin protein P2 in the nervous system. J Neurochem 1984; 42: 123–9.

Larkin MA, Blackshields G, Brown NP, Chenna R, McGettigan PA, McWilliam H, et al. Clustal W and Clustal X version 2.0. Bioinformatics 2007; 23: 2947–8.

Li H, Durbin R. Fast and accurate long-read alignment with Burrows-Wheeler transform. Bioinformatics 2010; 26: 589–95.

Majava V, Polverini E, Mazzini A, Nanekar R, Knoll W, Peters J, et al. Structural and functional characterization of human peripheral nervous system myelin protein P2. PLoS One 2010; 5: e10300.

McKenna A, Hanna M, Banks E, Sivachenko A, Cibulskis K, Kernytsky A, et al. The Genome Analysis Toolkit: a MapReduce framework for analyzing next-generation DNA sequencing data. Genome Res 2010; 20: 1297–303.

Murphy SM, Herrmann DN, McDermott MP, Scherer SS, Shy ME, Reilly MM, et al. Reliability of the CMT neuropathy score (second version) in Charcot-Marie-Tooth disease. J Peripher Nerv Syst 2011; 16: 191–8.

Nicholson G, Myers S. Intermediate forms of Charcot-Marie-Tooth neuropathy. Neuromol Med 2006; 8: 123–30.

Rotthier A, Auer-Grumbach M, Janssens K, Baets J, Penno A, Almeida-Souza L, et al. Mutations in the SPTLC2 subunit of serine palmitoyltransferase cause hereditary sensory and autonomic neuropathy type I. Am J Hum Genet 2010; 87: 513–22.

Ruskamo S, Yadav RP, Sharma S, Lehtimäki M, Laulumaa S, Aggarwal S, et al. Atomic resolution view into the structure-function relationships of the human myelin peripheral membrane protein P2. Acta Crystallogr D Biol Crystallogr 2014; 70: 165–76.

Saporta ASD, Sottile SL, Miller LJ, Feely SME, Siskind CE, Shy ME. Charcot-marie-tooth disease subtypes and genetic testing strategies. Ann Neurol 2011; 69: 22–33.

Scherer SS, Wrabetz L. Molecular mechanisms of inherited demyelinating neuropathies. Glia 2008; 56: 1578–89.

Scherer SS. The debut of a rational treatment for an inherited neuropathy? J Clin Invest 2011; 121: 4624–7.

Trapp BD, Dubois-Dalcq M, Quarles RH. Ultrastructural localization of P2 protein in actively myelinating rat Schwann cells. J Neurochem 1984; 43: 944–8.

Zenker J, Stettner M, Ruskamo S, Domènech-Estévez E, Baloui H, Médard J-J, et al. A role of peripheral myelin protein 2 in lipid homeostasis of myelinating Schwann cells. Glia 2014; 62: 1502–12.